doi:10.1111/j.1558-5646.2011.01416.x

CONVERGENT EVOLUTION OF PHENOTYPIC INTEGRATION AND ITS ALIGNMENT WITH MORPHOLOGICAL DIVERSIFICATION IN CARIBBEAN *ANOLIS ECOMORPHS*

Jason J. Kolbe,[1,2] Liam J. Revell,[3] Brian Szekely,[4] Edmund D. Brodie III,[5] and Jonathan B. Losos[1]

[1]Department of Organismic and Evolutionary Biology and Museum of Comparative Zoology, Harvard University, 26 Oxford St., Cambridge, Massachusetts 02138

[2]E-mail: jjkolbe@gmail.com

[3]National Evolutionary Synthesis Center, 2024 W. Main St., Durham, North Carolina 27705

[4]Massachusetts General Hospital, Center for Regenerative Medicine, 185 Cambridge St., Boston, Massachusetts 02114

[5]Mountain Lake Biological Station and Department of Biology, University of Virginia, Charlottesville, Virginia 22904

Received March 19, 2010
Accepted June 22, 2011
Data Archived: Dryad doi:10.5061/dryad.1d24c

The adaptive landscape and the G-matrix are keys concepts for understanding how quantitative characters evolve during adaptive radiation. In particular, whether the adaptive landscape can drive convergence of phenotypic integration (i.e., the pattern of phenotypic variation and covariation summarized in the P-matrix) is not well studied. We estimated and compared P for 19 morphological traits in eight species of Caribbean *Anolis* lizards, finding that similarity in P among species was not correlated with phylogenetic distance. However, greater similarity in P among ecologically similar *Anolis* species (i.e., the trunk-ground ecomorph) suggests the role of convergent natural selection. Despite this convergence and relatively deep phylogenetic divergence, a large portion of eigenstructure of P is retained among our eight focal species. We also analyzed P as an approximation of G to test for correspondence with the pattern of phenotypic divergence in 21 Caribbean *Anolis* species. These patterns of covariation were coincident, suggesting that either genetic constraint has influenced the pattern of among-species divergence or, alternatively, that the adaptive landscape has influenced both G and the pattern of phenotypic divergence among species. We provide evidence for convergent evolution of phenotypic integration for one class of *Anolis* ecomorph, revealing yet another important dimension of evolutionary convergence in this group.

KEY WORDS: Adaptive radiation, common principal components analysis, convergent evolution, genetic constraint, Mantel test, phenotypic variance–covariance matrices, random skewers.

Phenotypic diversification for quantitative traits during an adaptive radiation can be viewed as the result of the interplay between two multivariate processes, the multidimensional adaptive landscape and the **G**-matrix (Arnold et al. 2001, 2008). The adaptive landscape is a function relating the mean fitness of a population to the phenotypic trait means. The shape of the landscape represents underlying evolutionary features, such as correlational, stabilizing, or disruptive selection, and reveals where small fitness changes per unit of trait change exist, resulting in multivariate axes where peak movement is likely, termed the "selective lines of least resistance" (Arnold et al. 2001). It also clearly predicts how peak movement within the landscape induces directional selection and how the curvature and orientation of a moving peak generates nonlinear selection. In contrast, long-term stability of

peak position promotes evolutionary stasis via stabilizing selection. Moreover, convergent phenotypic evolution may occur if a similar topology of the adaptive landscape exists in different geographic locations.

Phenotypic evolution over short timescales depends both on the position of a population within an adaptive landscape and the pattern of inheritance for multiple traits. This pattern of inheritance is usually summarized in the **G**-matrix, a square symmetric matrix composed of additive genetic variances for traits on the diagonal and covariances elsewhere (Lande 1979; Arnold 1992; Lynch and Walsh 1998). Covariances among characters can play an important role in shaping the course of evolution by natural selection (Schluter 1996; Arnold et al. 2001). The multivariate response to selection equation, $\Delta\bar{\mathbf{z}} = \mathbf{G}\mathbf{P}^{-1}\mathbf{s}$, summarizes how genetic patterns of trait covariance translate natural selection into phenotypic evolution (Lande 1979; Lande and Arnold 1983; Björklund 1996). In this equation, $\Delta\bar{\mathbf{z}}$ is the vector of change in phenotypic mean trait values, **P** is a matrix containing the phenotypic variances and covariances, and **s** is the vector of selection differentials (Lande 1979).

Under most conditions, **G** will tend to bias the response to selection away from the direction maximizing the increase in mean fitness, summarized in the selection gradient ($\boldsymbol{\beta} = \mathbf{P}^{-1}\mathbf{s}$), and represented in the adaptive landscape as the steepest uphill direction relative to the position of a population. The phenotypic response to selection ($\Delta\bar{\mathbf{z}}$) will generally not be collinear with $\boldsymbol{\beta}$ for most conditions of **G** (Lande and Arnold 1983; Arnold 1992; Björklund 1996). Rather it will be biased toward the major eigenvector of **G**, the direction of greatest genetic variation ($\mathbf{g}_{\max}$), termed the genetic "line of least resistance" (Schluter 1996). This bias creates a curved evolutionary trajectory as the population approaches a local adaptive optimum and is expected to diminish over time (Lande 1980a; Björklund 1996; Schluter 1996, 2000; Arnold et al. 2001). Thus, evolutionary divergence of phenotypic characters represents a balance between the effects of natural selection, in the form of the adaptive landscape, and those of genetic constraint in the form of additive genetic variances and covariances (Lande 1979; Björklund 1996; Schluter 1996, 2000; Arnold et al. 2001; Blows et al. 2004).

Multivariate selection imposed by the adaptive landscape is also expected to modify elements of **G** (Lande 1980b, 1984; Cheverud 1984; Arnold 1992; Brodie 1992; Arnold et al. 2001, 2008; Jones et al. 2003; Blows et al. 2004; Revell 2007a). Although **G** is expected to be stable under some circumstances, it also may be quite unstable under others (Turelli 1988; Agrawal et al. 2001; Arnold et al. 2001, 2008; Phillips et al. 2001; Steppan et al. 2002; Jones et al. 2003; Björklund 2004; Revell 2007a). In particular, simulation studies show large effective population sizes enhance stability of the size, shape, and orientation of **G** (Jones et al. 2003). Furthermore, correlated pleiotropic mutation, strong correlational selection, and directional selection promote stability in the orientation of **G** (Jones et al. 2003, 2004), and empirical studies show correlational selection tends to cause genetic covariances to evolve in the direction of the sign of the correlation (Cheverud 1984; Tallis and Leppard 1988; Brodie 1992; Blows et al. 2004; McGlothlin et al. 2005). These expected patterns of response to selection lead to the prediction that species experiencing similar multivariate selection regimes will converge in genetic architecture, but this hypothesis has seldom been tested empirically (but see Marroig and Cheverud 2001; Roff 2002).

Comparative studies of phenotypic integration (**P**) can offer important insight into patterns of multivariate phenotypic evolution (e.g., Steppan 1997; Game and Caley 2006), and data from multiple species are needed to test patterns of divergence and convergence of **P** among species. Furthermore, if **P** and **G** are related, analysis of **P** can provide insight into the underlying genetic architecture. Comparative data for **G** are difficult to obtain because estimating genetic parameters requires large-scale breeding experiments or natural pedigrees, and even under ideal circumstances **G** is often inferred with large error. However, some evidence suggests that **P** can often be a reasonable approximation for **G** in evolutionary studies (Cheverud 1988, 1996; Roff 1995; Steppan et al. 2002). Because $\mathbf{P} = \mathbf{G} + \mathbf{E}$ (the matrix of environmental variances and covariances), **G** and **P** should often be correlated (Cheverud 1988; Roff 1995, 1997), particularly if heritabilities are high such as is found for many morphological traits like those in this study (Roff 1997, but see Hadfield et al. 2007). Furthermore, because the sample size for **P** is the number of individuals, whereas the effective sample size for **G** is a function of the number of families in the breeding experiment, **P** can usually be estimated with smaller error than can **G**. This has led to the argument that sometimes a precise measure of **P** might be closer to the "true" **G** than a genetic estimate made with large error (Cheverud 1988, 1996). Additionally, many "nonmodel" species are not amenable to breeding in the laboratory, so empirical estimates of **G** for multiple species can be difficult to obtain. For these reasons, we use **P** as a first approximation of **G** for some evolutionary inferences of this study, including testing for an effect of genetic architecture on phenotypic divergence. Objections to this approach have been raised on both empirical and theoretical grounds (see Willis et al. 1991); however, we argue that our substitution of **P** for **G** in species divergence comparisons is more likely to increase the type II rather than the type I error probability of those tests.

ANOLIS LIZARDS

To better understand the nature of phenotypic integration as an adaptation to ecological conditions and as a possible constraint on the pattern of divergence among species (Merilä and Björklund 2004), a comparative study of multiple, phenotypically divergent species with a robust phylogeny is needed

(Steppan et al. 2002). Lizards in the genus *Anolis*, or anoles, are a model system for studying adaptive radiation (Schluter 2000; Losos 2009). Nearly 400 morphologically and ecologically diverse species exist in North, Central, and South America with more than 150 species known from Caribbean islands alone. A well-supported phylogenetic hypothesis exists for much of the genus (Nicholson et al. 2005; Mahler et al. 2010) and a reasonable estimate for the age of the radiation is 40 million years (Losos 2009). The Caribbean species are particularly well studied, in part due to the repeated evolution of similar habitat specialists, or "ecomorphs" (Williams 1972), on the different islands of the Greater Antilles. Ecomorphs are ecological analogs, which in most cases independently evolved on each of the four Greater Antillean islands—Cuba, Hispaniola, Jamaica, and Puerto Rico—and are named for the structural microhabitat they most often occupy, such as grass-bush, trunk-ground, or twig (Williams 1983; reviewed in Losos 2009). These ecomorphs are morphologically distinct from each other and similar among islands (Losos 2009).

Multivariate phenotypic convergence has been explored extensively in this group (e.g., Losos 1990; Butler and Losos 2002; Harmon et al. 2005; Langerhans et al. 2006; Johnson et al. 2010). Independently evolved ecomorphs are convergent for several functionally distinct sets of morphological characters, including body size, body shape, head shape, lamella number, and sexual-size dimorphism, but the pattern of convergence differs among these character sets (Harmon et al. 2005). In light of the extensive ecological studies on anoles and the observed convergence in morphology of *Anolis* ecomorphs (reviewed in Losos 2009), measures of phenotypic integration from ecologically similar, but relatively distantly related species provide a test for the convergence of **P** driven by natural selection. Only one prior study examined genetic constraints as a possible determinant of the pattern of differentiation of anoles and that study focused on differentiation among populations of a single species (Revell et al. 2007). Thus, the role of genetic architecture and the adaptive landscape in the phenotypic diversification of Caribbean *Anolis* species remains untested.

We focus on three questions about morphological evolution in Caribbean *Anolis* lizards. First, does the pattern of phenotypic variation and covariation (**P**) differ among habitat specialists (ecomorphs), and do similarities in the selection regime (i.e., ecomorph class) lead to convergence of **P**? Second, do some functionally based character sets (e.g., limbs) show stronger integration than others, and does the pattern of integration vary among species? For these two questions, we analyze **P**-matrices estimated for eight species of *Anolis* lizards as a measure of phenotypic integration. Third, does genetic architecture within species influence the pattern of phenotypic divergence among species? Here, we invoke Cheverud's conjecture (Cheverud 1988; Roff 1995), using **P** as an approximation of **G**, and analyze data from 21 *Anolis* species in the six ecomorph classes. Alignment with **P** would indicate that genetic constraint and/or a persistent shape of the adaptive landscape influence the pattern of phenotypic divergence (Arnold et al. 2008). The latter case would indicate that the adaptive landscape influences both **P** and the pattern of divergence among species.

Materials and Methods

SPECIMENS AND MORPHOLOGICAL MEASUREMENTS

We examined 769 museum specimens from eight *Anolis* species (Fig. 1) representing each ecomorph on Hispaniola: *A. baleatus* (crown-giant; $n = 83$), *A. chlorocyanus* (trunk-crown; $n = 95$), *A. cybotes* (trunk-ground; $n = 97$), *A. distichus* (trunk; $n = 102$), *A. insolitus* (twig; $n = 39$), and *A. semilineatus* (grass-bush; $n = 100$), as well as two additional trunk-ground species: *A. gundlachi* ($n = 79$) from Puerto Rico and *A. sagrei* ($n = 174$) from Florida (native primarily to Cuba; Kolbe et al. 2004, 2007). We chose museum specimens to minimize the number of localities for each species while still obtaining a reasonable sample size for **P**-matrix estimation; however, for one species, *A. insolitus*, which is less common in collections due to its lower population density and greater crypticity, we measured all available museum specimens. In addition to these eight species, we included data for 13 additional species from Harmon et al. (2005) for analyses involving species means, including one representative species from each ecomorph-island combination (i.e., six ecomorphs and four islands: trunk ecomorphs do not occur on Puerto Rico or Jamaica and grass-bush anoles do not occur on Jamaica; Losos 2009). We obtained the phylogenetic trees used in analyses by pruning the phylogeny of Nicholson et al. (2005).

We measured morphological traits previously shown to distinguish *Anolis* ecomorphs and that are ecologically relevant to anoles (reviewed in Losos 2009). For each specimen, we used a metric ruler to measure snout-vent length (SVL) from the tip of the snout to the cloacal opening and calipers to measure head length, head width, head height, and the length and width of the toe pads on the third toe of the forelimb and the fourth toe of the hindlimb. We also obtained radiographs for all specimens to measure the following skeletal elements using the computer-driven imaging system MorphoSys (Meacham 1993): humerus, ulna, femur, tibia, first phalanx on the third toe of the forefoot, first and second phalanges on the fourth toe of the hindfoot, pelvic width, and pectoral width. We also counted the number of lamellae on the second and third phalanges of both the third toe of the forelimb and the fourth toe of the hindlimb with a dissecting scope. We measured each specimen twice to check for consistency. We repeated any measurement differing by more than 5% and then averaged values for each specimen. We collected all

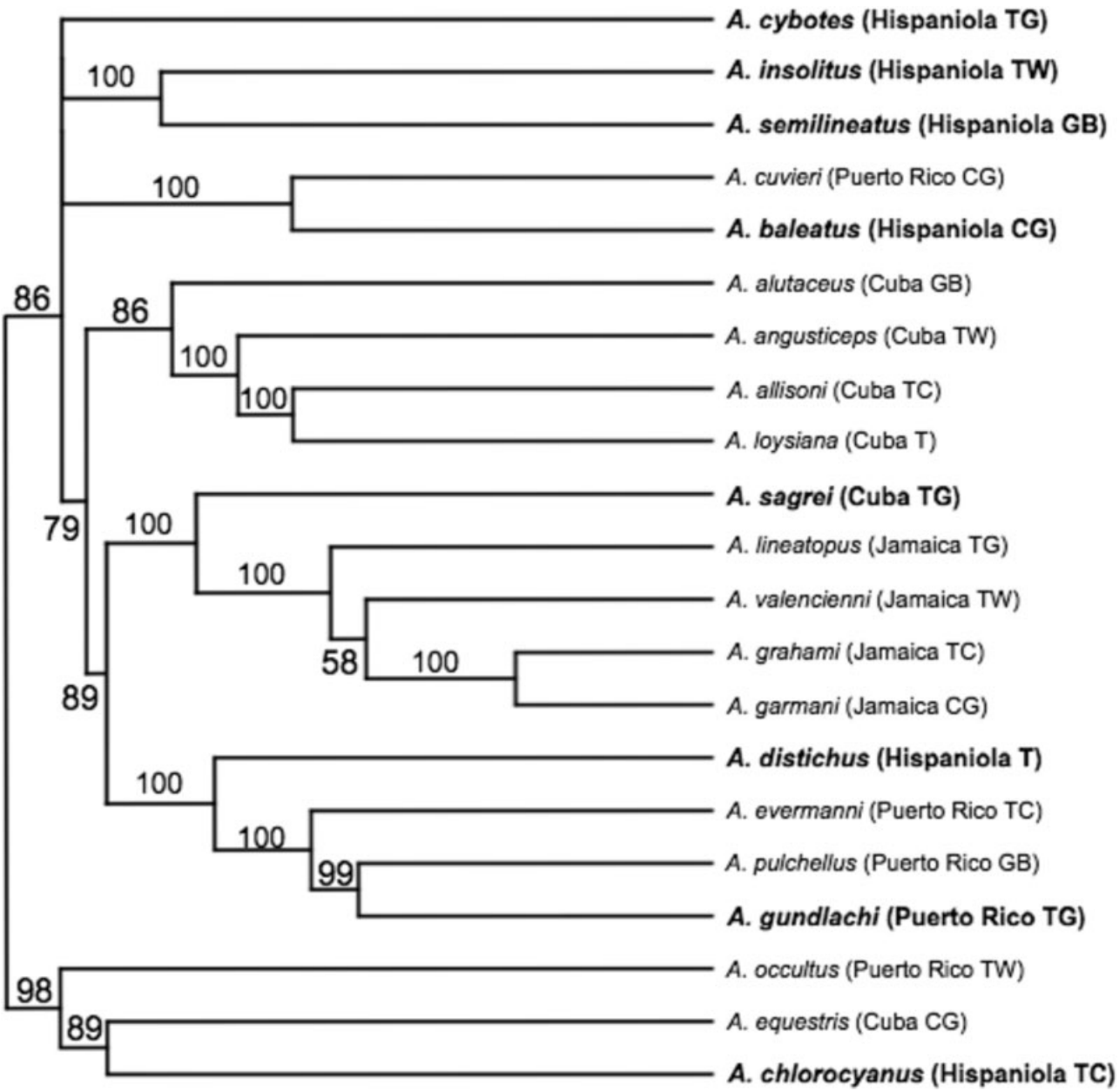

Figure 1. Phylogenetic tree used in this study, which was obtained by pruning the phylogeny Nicholson et al. (2005) to include the 21 species analyzed in this study. The distance from the root to the tips was arbitrarily set to unit length. Recent estimates date the root of the *Anolis* tree at approximately 40 million years (see Losos 2009 for details). For each species, island and ecomorph category are indicated in parentheses (CG = crown-giant, GB = grass-bush, T = trunk, TC = trunk-crown, TG = trunk-ground, and TW = twig). The eight focal species in the P-matrix study are in bold. Bayesian posterior probabilities (in %) are given above each node except when < 50%, in which case the node was collapsed into a multifurcation.

measurements in millimeters (mm), with the exception of lamella counts. Our final dataset thus consisted of 19 morphological traits for the eight focal species. The species means dataset derived from the eight species in this study and 13 additional species from Harmon et al. (2005), which included only 15 of these morphological traits because data for the length and width of the toe pads on the third toe of the forelimb and the fourth toe of the hindlimb were not collected.

MULTIVARIATE MORPHOLOGICAL DIFFERENCES

To test for morphological differences among species and ecomorphs, we conducted multivariate analyses of covariance (MANCOVA) with SVL as a covariate. These analyses did not take into account phylogenetic relationships among species, and were conducted simply to establish that multivariate patterns of divergence and convergence for species sampled in this study are consistent with previous analyses of *Anolis* ecomorphs (Losos 1990;

Harmon et al. 2005; Langerhans et al. 2006). First, we tested the hypothesis that the eight focal species differed in morphology using the dataset of 18 morphological traits and SVL as a covariate. Second, we tested for differences among the six ecomorph classes using species means data for all 21 species (Harmon et al. 2005 and this study). This MANCOVA used the dataset of 14 morphological traits and SVL as a covariate. All variables were natural logarithm (log) transformed prior to analysis, which were conducted with JMP 8.0.2 (JMP 2009).

P-MATRIX COMPARISONS

To estimate **P**, our measure of phenotypic integration, we calculated phenotypic correlation and variance–covariance (VCV) matrices for each species using log-transformed data. To remove effects of mean differences among collecting localities for each of the eight species, we conducted MANCOVAs using the datasets of 18 morphological traits and SVL as a covariate. The partial correlation and VCV matrices from these MANCOVAs were used in subsequent analysis of **P**, the phenotypic correlation and VCV matrices, respectively. These **P**-matrices were pooled for species divergence comparisons and analyzed with the species mean dataset for 21 *Anolis* species (see Species Divergence Comparisons).

We employed both matrix similarity tests and common principal components analysis (CPCA) to assess the overall level of similarity in **P** and identify the level of shared eignestructure among species (Steppan 1997; Ackermann and Cheverud 2000; Game and Caley 2006). We conducted Mantel tests to determine the overall similarity between phenotypic correlation matrices of each species pair (Mantel 1967). This method tested the null hypothesis of no similarity between phenotypic correlation matrices and provided a value for each matrix correlation (r_M). We calculated the *P*-value of the test statistic by randomly permuting rows and columns together of one matrix 9999 times for each comparison (Mantel 1967). For each permutation, we calculated a pseudo-value of the matrix correlation (r_M'). We then evaluated the *P*-value of the matrix correlation by computing the relative frequency of $r_M' \geq r_M$.

Because Mantel tests can only be applied to matrices with diagonals composed of either zeros or ones (such as correlation matrices; Dietz 1983), we used random skewers (Cheverud et al. 1983; Cheverud 1996; Revell 2007a; Revell et al. 2007) to test for similarity in phenotypic VCV matrices. This pairwise approach multiplies each VCV matrix by a random selection vector and calculates the vector correlation coefficient (r_S) between the resulting response vectors (Revell 2007a). The test statistic is the mean value of r_S calculated from 10,000 random selection vectors and its significance is determined by comparison to the expected distribution of correlations between randomly generated vectors (Cheverud 1996). As with our Mantel tests on the correlation matrices, the null hypothesis of random skewers is no similarity between phenotypic VCV matrices.

In addition to these measures of overall matrix similarity provided by r_M and r_S, we also used CPCA to determine the level of shared eigenstructure among phenotypic VCV matrices (Flury 1987; Phillips and Arnold 1999). In CPCA, we evaluated a hierarchical set of models for similarity in the eigenstructure of two VCV matrices: ranging from no shared eigenvectors, to some or all shared eigenvectors, to shared eigenvectors and eigenvalues. To determine the level of shared eigenstructure between each pair of VCV matrices, we used the best-fit model approach as implemented by Phillips and Arnold (1999). In this approach, we calculated Akaike information criteria (AIC) values for each model of matrix similarity. AIC is a model selection criterion that balances the goodness of fit of a model against the number of parameters, and the lowest AIC value indicates the best-fitting model (Akaike 1973; Burnham and Anderson 2002). We also calculated Akaike weights for all models in each matrix comparisons and estimated 95% confidence limits around our selected model using the estimated weights (Burnham and Anderson 2002; Game and Caley 2006). Matrix correlations and CPCA test different hypotheses (Steppan 1997; Ackermann and Cheverud 2000; Cheverud and Marroig 2007) and we view them as complementary approaches.

To test for a relationship between phylogenetic history and similarity in **P**, we compared a matrix of patristic distances (i.e., the sum of the branch lengths between each pair of species; Farris 1967) for the eight focal species to matrices of correlation values from Mantel tests (r_M) and random skewers (r_S). We obtained patristic distances from the most complete *Anolis* phylogeny available (Nicholson et al. 2005; Fig. 1). In addition to testing for a phylogenetic effect on matrix similarity, we evaluated the hypothesis that the three trunk-ground species in the present study are more similar in **P** than species pairs belonging to different ecomorph classes. We performed this test by comparing correlations (r_M and r_S) and the number of shared common principal components (AIC model selection criterion) between species pairs that belong to either the same or different ecomorph using Wilcoxon tests.

PATTERN OF AMONG-TRAIT PHENOTYPIC INTEGRATION

We analyzed all traits together to evaluate overall similarity of **P** among *Anolis* species and to test for convergence of **P** within an ecomorph class. Similarity of **P** in different species suggests that these species show similar patterns of phenotypic integration, but not all traits are expected to show similar covariances and species may vary in their degree of integration. Morphological integration can arise due to shared functional or developmental processes, common inheritance via linkage disequilibrium

or pleiotropy, or the coordinated evolution of elements within a functional unit (Olson and Miller 1958; Chernoff and Magwene 1999; Marroig and Cheverud 2001). Thus, some sets of traits may be more tightly integrated than others, and the strength of integration may vary among species; an aspect of integration not captured by overall comparisons of **P**. We explored how patterns of phenotypic integration in different subsets of characters vary among species.

We used a series of correlation analyses to assess the relative strength of phenotypic integration among character sets and how this varies among species. A prior study of *Anolis* ecomorphs identified different patterns of convergence among character sets, such as body size, head shape, body shape, and lamellae (Harmon et al. 2005). Furthermore, variation among ecomorph classes suggests that each character set represents an adaptation to a different aspect of the environment. Thus, we hypothesize that traits within each of these character sets may coevolve as a functional unit, experiencing correlational selection that results in stronger integration with other traits within a set. We tested for integration of character sets using the estimated phenotypic correlation matrices (**P**) for each species, and design matrices describing each morphological character set. We constructed these design matrices by entering a one in the matrix if the two traits belonged to the same character set and a zero otherwise. We computed a Mantel matrix correlation to determine if the phenotypic correlation and design matrices were related (Cheverud 1995, 1996) using six design matrices that included every combination of the three character sets (i.e., head-limbs-lamellae; head-limbs; head-lamellae; limbs-lamellae; head; limbs; and lamellae). Comparing across these separate matrix correlations tests whether each set of characters increases or decreases the strength of phenotypic integration. We specified the character sets as follows: limbs (humerus, ulna, first phalanx on the third toe of the forefoot, femur, tibia, and first and second phalanges on the fourth toe of the hindfoot), head shape (head length, head width, and head height), and lamellae (number of lamellae on the second and third phalanges of both the third toe of the forelimb and the fourth toe of the hindlimb) corresponding to Harmon et al. (2005).

SPECIES DIVERGENCE COMPARISONS

We used **P** as an approximation of **G** to determine if the pattern of divergence among *Anolis* species was coincident with within-species phenotypic VCV. We tested for a correlation between the pooled phenotypic VCV matrix (pooled **P)** and the among species VCV matrices, **D** or $\mathbf{D_{IC}}$, in which the latter among species matrix incorporates phylogenetic information (Merilä and Björklund, 1999; Baker and Wilkinson 2003; Bégin and Roff 2003, 2004; Blows and Higgie 2003; Marroig et al. 2004; McGuigan 2006; Revell 2007b). We calculated pooled **P** by taking the weighted mean of **P** for the eight focal species, with weights proportional to the sample size of each species (Manly 2005). This procedure corrects for mean differences among species while calculating the best estimate of **P** for the *Anolis* species of our study. We estimated **D**, the VCV matrix of species means, and $\mathbf{D_{IC}}$, a phylogenetically corrected among species VCV matrix computed from independent contrasts (Felsenstein 1985; Baker and Wilkinson 2003; Revell 2007b; Revell and Harmon 2008), using species means for all 21 species (Fig. 1). We tested for correlations between pooled **P** and **D** or $\mathbf{D_{IC}}$ using Mantel tests and random skewers. Measurement error could affect these results, but Revell et al. (2007) showed that for comparisons of similar traits among populations of *A. cristatellus*, correlations were significantly greater than expected by sampling error (assessed by a randomization procedure). Furthermore, variability among species means in this study is much larger than the variability within a species in that study, suggesting measurement error will have little effect in our study. Significant correlations in these tests show that the pattern of within-species VCV in *Anolis* is coincident with the pattern of phenotypic divergence among species.

Marroig and Cheverud (2004) present a series of tests derived from quantitative genetic theory to determine the importance of natural selection and genetic drift for multivariate morphological evolution. Proportionality of within and among species VCV matrices is expected under genetic drift (Lande 1979). Rejecting the null hypothesis of genetic drift for morphological evolution might then provide evidence of diversifying or stabilizing selection. However, failure to reject this null hypothesis is not definitive evidence of the absence of natural selection, they therefore also present a test for evidence of a correlated response of trait combinations to selection. Using pooled **P** for our within-species VCV matrix, as calculated above, we first reduced this matrix to its principal components. We next computed the principal component scores of each multivariate species mean by projecting that species mean into the eigenspace of our pooled **P** matrix. For each eigenvector in the eigenspace of the pooled **P** matrix, we then computed the variance in the principal component scores from the species means. Under pure genetic drift, the variance among species on each eigenvector of the pooled **P** matrix should be directly proportional to the corresponding eigenvalue of **P** (Lande 1979). Thus, to test for evolution by selection, we then performed a log–log regression of the eigenvalues of **P** and the corresponding among species variances in species means, and tested for a significant deviation of the regression slope from 1. The expectation is that a significant deviation indicates the pattern of among species divergence is unlikely to have occurred by drift with interpretations of diversifying and stabilizing selection on particular PC axes dependent on whether the regression slope is greater or less than 1 (Marroig and Cheverud 2004). We conducted this analysis using both the untransformed species means data and

independent contrasts (the latter to control for phylogenetic relationships among species).

To test for correlational selection, we computed the VCV matrix of the principal component scores of the species means in the eigenspace of pooled **P**. Under genetic drift, the scores of the species means in the eigenspace of **P** should be uncorrelated (Marroig and Cheverud 2004). Alternatively, significant correlations between the principal component scores of the species means suggest a correlated response of the eigenvectors of **P** to selection. This test does not rely on interpreting these PC scores as biologically meaningful traits, only that selection on the original traits results in a detectable departure from sphericity of the among species VCV matrix in the eigenspace of **P**. We used the Bartlett χ^2 test to evaluate the overall significance of the correlation among PC scores with significant result causing us to reject the null hypothesis of genetic drift (Marroig & Cheverud 2004). As before, we conducted this analysis as described here for untransformed species means and independent contrasts. We adjusted *P*-values for multiple comparisons (Rice 1989), and report results for both corrected and uncorrected *P*-values.

Results

MULTIVARIATE MORPHOLOGICAL DIFFERENCES

The overall difference in the vector of mean morphological values differs significantly among the eight focal species (MANCOVA: Wilks' $\lambda = 0.00003$, $P < 0.0001$; Fig. 2), and univariate ANCOVAs for the 18 morphological traits are significant (all $P < 0.0001$). In the 21-species dataset, the ecomorph classes are also significantly different from each other in morphology (MANCOVA: Wilks' $\lambda = 0.000003$, $P = 0.018$; Fig. 2), and all univariate ANCOVAs for the 14 morphological traits are significant at $P < 0.0001$. These multivariate results are consistent with previous studies of *Anolis* ecomorphs.

P-MATRIX COMPARISONS

We find significant similarity in **P** among the eight focal *Anolis* species (Table 1; Fig. 3). Mantel correlations (r_M) for phenotypic correlation matrix comparisons range from 0.28 to 0.79 for pairwise comparisons, whereas random skewers correlations (r_S) for phenotypic VCV comparisons are somewhat higher, ranging from 0.67 to 0.93. Because tests on VCV matrices can be affected by the scale of the original variables, we removed lamella count traits and repeated the random skewers analyses. We obtained virtually identical correlation values in each case. No relationship exists between patristic distance from the phylogeny and similarity in **P** (Mantel correlations, $r_M = 0.17$, $P = 0.53$; random skewers; $r_S = 0.19$, $P = 0.55$; Fig. 3). Matrix correlations among the three trunk-ground species are higher than correlations obtained from pairs of species belonging to different ecomorph classes (Wilcoxon tests, r_M: $z = 2.45$, $P = 0.007$, one-tailed; r_S: $z = 1.75$, $P = 0.040$, one-tailed; Table 1).

Although all the matrix correlations are statistically significant, results show variation among species in **P** similarity; likewise, CPCA reveal some variation among species in the degree of shared phenotypic eigenstructure (Table 2). The results of pairwise comparisons of phenotypic VCV matrices range from sharing six eigenvectors to full CPC (i.e., all 18 eigenvectors shared, but eigenvalues not proportional between matrices). Representatives from the same ecomorph class (all trunk-ground anoles in this case) share all principal components, which is significantly

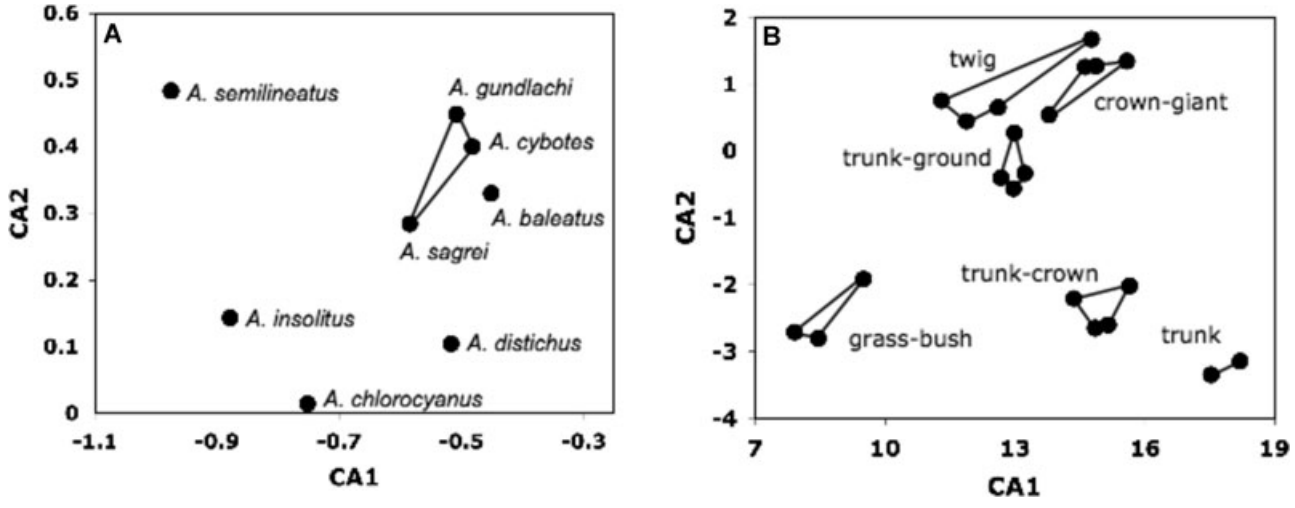

Figure 2. Plots of canonical axes 1 and 2 from two separate MANCOVAs using (A) the eight species in the P-matrix study (lines connect the three trunk-ground species: *Anolis cybotes*, *A. gundlachi*, and *A. sagrei*) and (B) the 21 species in *Anolis* ecomorph divergence study (lines connect members of a common ecomorph class).

Table 1. Results of Mantel (r_M, above diagonal) and random skewers (r_S, below diagonal) tests for pairwise correlations between P-matrices (phenotypic correlation and VCV matrices, respectively) estimated for each species and all species together (pooled P, see text for details on its calculation). Significance levels are $P < 0.01$ for all correlations based on random permutations. Ecomorph category is indicated in parentheses (CG = crown-giant, GB = grass-bush, T = trunk, TC = trunk-crown, TG = trunk-ground, and TW = twig). Trunk-ground species and their pairwise correlation values are bold.

	A. baleatus	*A. chlorocyanus*	***A. cybotes***	*A. distichus*	***A. gundlachi***	*A. insolitus*	***A. sagrei***	*A. semilineatus*	Pooled **P**
A. baleatus (CG)		0.673	0.657	0.502	0.608	0.335	0.713	0.595	0.800
A. chlorocyanus (TC)	0.782		0.682	0.563	0.645	0.384	0.747	0.623	0.843
***A. cybotes* (TG)**	0.862	0.790		0.519	**0.667**	0.507	**0.786**	0.666	0.865
A. distichus (T)	0.859	0.858	0.876		0.558	0.278	0.548	0.576	0.710
***A. gundlachi* (TG)**	0.725	0.665	**0.840**	0.790		0.422	**0.784**	0.565	0.842
A. insolitus (TW)	0.701	0.725	0.829	0.783	0.839		0.428	0.398	0.535
***A. sagrei* (TG)**	0.846	0.802	**0.927**	0.890	**0.877**	0.840		0.634	0.923
A. semilineatus (GB)	0.823	0.797	0.888	0.891	0.771	0.781	0.887		0.787
Pooled **P**	0.888	0.868	0.950	0.950	0.882	0.865	0.965	0.947	

more than species pairs belonging to different ecomorph classes (Wilcoxon test on the number of shared principal components, AIC: $z = 1.92$, $P = 0.027$, one-tailed; Table 2) and is consistent with the correlation-based analyses.

PATTERN OF AMONG-TRAIT PHENOTYPIC INTEGRATION

Matrix correlations between species' phenotypic correlation matrices (**P**) and our design matrices show evidence of significant phenotypic integration in limbs for all species and head shape for some species (Table 3). Toe pad lamellae, by contrast, did not show evidence of phenotypic integration. Limb traits are consistently more integrated than head characters for all species except *A. insolitus* and *A. semilineatus*, which have the highest correlation values for head shape integration. The three trunk-ground species have the highest correlation values for limb integration (Table 3). Overall, inclusion of head and limb traits increases the strength of integration, whereas when lamellae are included the strength of integration changes only slightly. Trait pairs within the same character set (e.g., humerus-femur) show tighter positive correlations than traits in different character sets (e.g., lamellae fourth-femur; Fig. 3).

SPECIES DIVERGENCE COMPARISONS

Pooled **P** is significantly correlated with **D**, the VCV matrix of species means uncorrected for phylogeny (Mantel test: $r_M = 0.74$, $P = 0.0003$; random skewers: $r_S = 0.71$, $P = 0.0011$). Principal component eigenvectors for pooled **P** are shown in Table 4, along with associated eigenvalues. With the phylogeny taken into account by computing the species divergence matrix from independent contrasts ($\mathbf{D_{IC}}$), the correlation between pooled **P** and $\mathbf{D_{IC}}$ is almost identical in strength to the nonphylogenetic correlation (Mantel test: $r_M = 0.73$, $P = 0.0001$; random skewers: $r_S = 0.73$, $P = 0.0006$; Fig. 4). This suggests our findings are robust to standard phylogenetic assumptions, such as Brownian motion. Furthermore, these highly significant correlation results suggest that our substitution of **P** for **G** did not lead to tests with poor sensitivity (i.e., prone to Type II error).

When evaluating evidence for selection, the regression tests of among-species variances on within-species eigenvalues (from pooled **P**) show no significant difference from a slope of 1 using both species means ($\beta = 1.20$, $P = 0.28$, 95% CI: $0.43 < \beta < 1.97$) and independent contrasts ($\beta = 1.19$, $P = 0.26$, 95% CI: $0.50 < \beta < 1.88$), and variances in no PC dimension deviate significantly from the regression line. Thus, drift cannot be rejected in these regression analyses. However, when these regression tests are restricted to the first six eigenvalues, the minimum number of eigenvectors shared among the eight focal species as detected by CPCA, the slope for species means is significantly greater than 1 ($\beta = 1.76$, $P = 0.02$, 95% CI: $0.59 < \beta < 2.94$) and the independent contrasts slope is only marginally nonsignificant ($\beta = 1.69$, $P = 0.06$, 95% CI: $0.19 < \beta < 3.19$). This shows one or more of the first few PCs are more variable than expected under genetic drift, which could occur through diversifying selection on highly variable PC axes or stabilizing selection on other PC axes (Marroig and Cheverud 2004). Furthermore, the Bartlett χ^2 test of probabilities for PC score correlations is highly significant using both species means and independent contrasts (Table 5), rejecting drift and showing a correlated response of some PC axes to selection. Twenty-five of 91 pairwise PC comparisons are correlated using species means (four of 91 after Bonferroni correction, which we consider to be excessively conservative) and 27 of 91 pairwise PC comparisons are correlated using independent contrasts (five of 91 after Bonferroni correction; Table 5). Taken together, these results provide evidence for selection during the diversification of the species in our study. In particular, we found some

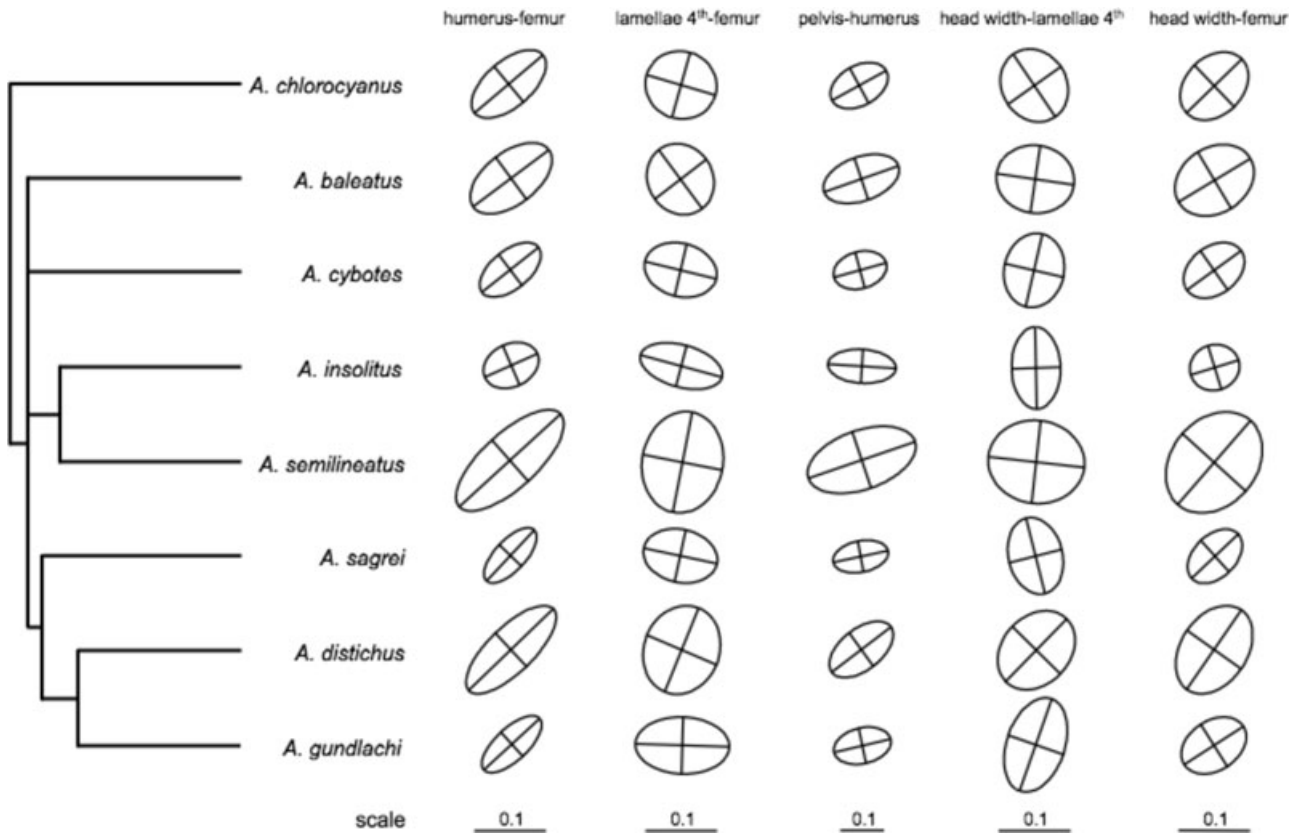

Figure 3. Phylogeny for the eight species in the P-matrix analysis along with ellipses representing the co-distribution of five trait pairs: humerus–femur, lamellae 4th-femur, pelvis width-humerus, head width-lamellae 4th, and head width-femur, all after adjusting for size. The length and width of each ellipse is proportional to two times the square root of the primary and secondary eigenvalue of the reduced variance–covariance matrix for the two focal traits, respectively, with the scale shown along the lower margin. The orientation of the ellipse is the orientation of the primary eigenvector.

evidence for diversifying selection on the major PC axes of **P** and/or stabilizing selection on the minor axes of **P**, and we found highly significant correlation selection among PC axes. However, because we conducted this analysis on the PC axes, which represent orthogonal linear combinations of our original traits, it is difficult to evaluate the form of selection on our originally measured traits (beyond rejecting drift). Furthermore, correlated evolution might be due to morphological traits evolving together via correlational selection or be produced by the direction of peak movement of an adaptive landscape (Arnold et al. 2008).

Discussion

We found evidence that patterns of covariation among traits are shaped by natural selection. Ecologically similar trunk-ground species are more similar in **P**, which suggests that not only are ecologically similar anole species convergent in morphological trait means, as previously documented (reviewed in Losos 2009; Fig. 2), but also in the pattern of integration underlying these same traits (Tables 1 and 2). Moreover, correlational selection was detected in our analysis of PC axes. Despite the apparent role of selection in driving this convergence of phenotypic integration, overall patterns of trait covariance are nonetheless aligned with among-species divergence patterns across the 40 million years of evolution estimated for the *Anolis* radiation (Losos 2009). We discuss these results in greater depth below.

SPECIES DIFFERENCES IN P

We found that similarity in **P** varied among species pairs (Tables 1 and 2), with some species pairs quite similar in **P** and others divergent. However, similarity of **P** was not correlated with phylogenetic relationship. In a similar study of **P** in leaf-eared mice (*Phyllotis*), Steppan (1997) also found no association between phylogeny and **P**, but there was a tendency for fewer shared components with more inclusive clades. We did find, however, evidence of greater **P**-matrix similarity among members of the same ecomorph class. In particular, the three ecologically similar trunk-ground species (*A. cybotes, A. gundlachi*, and *A. sagrei*) shared more similar covariance structure with each other than with species belonging to other ecomorph classes (Tables 1 and 2),

Table 2. Results of common principal components analyses of phenotypic VCV matrices using the AIC for the best-fit model selection procedure. The best-fitting model of matrix similarity based on AIC (above diagonal) and the 95% confidence limits for the Akaike weights (below diagonal) are shown for each pairwise comparison. Ecomorph category is indicated in parentheses (CG = crown-giant, GB = grass-bush, T = trunk, TC = trunk-crown, TG = trunk-ground, and TW = twig). Model abbreviations are CPC for the full common principal component model (i.e., all 18 eigenvectors shared but eigenvalues not proportional between matrices) and PCPC for partial common principal component model with the number of shared eigenvectors in parentheses. Trunk-ground species, their pairwise best-fit AIC model, and the 95% confidence limits for that model are bold.

	A. baleatus	*A. baleatus*	***A. cybotes***	*A. distichus*	***A. gundlachi***	*A. insolitus*	***A. sagrei***	*A. semilineatus*
A. baleatus (CG)		CPC	CPC	CPC	CPC	PCPC(11)	CPC	CPC
A. chlorocyanus (TC)	PCPC(15)-CPC		PCPC(16)	CPC	PCPC(16)	PCPC(6)	PCPC(16)	PCPC(9)
***A. cybotes* (TG)**	PCPC(15)-CPC	PCPC(15)-CPC		PCPC(9)	**CPC**	PCPC(14)	**CPC**	PCPC(8)
A. distichus (T)	PCPC(15)-CPC	PCPC(15)-CPC	PCPC(7–9)		PCPC(15)	PCPC(16)	PCPC(11)	PCPC(9)
***A. gundlachi* (TG)**	PCPC(15)-CPC	PCPC(14)-CPC	**PCPC(14)-CPC**	PCPC(14–15)-CPC		CPC	**CPC**	PCPC(6)
A. insolitus (TW)	PCPC(9–11), PCPC(15)-CPC	PCPC(6)	PCPC(8,9, 14–16)	PCPC(7,11), PCPC(14)- CPC	PCPC(15)-CPC		PCPC(16)	PCPC(12)
***A. sagrei* (TG)**	PCPC(13), PCPC(15)-CPC	PCPC(15)-CPC	**PCPC(14)-CPC**	PCPC(10–11), PCPC(15)-CPC	**PCPC(15)-CPC**	PCPC(13), PCPC(15)-CPC		PCPC(14)
A. semilineatus (GB)	PCPC(15)-CPC	PCPC(9,11), PCPC(14)-CPC	PCPC(8–9)	PCPC(8–10), PCPC(16)-CPC	PCPC(6)	PCPC(11–12), PCPC(14)-CPC	PCPC(14)	

Table 3. Morphological integration results showing the matrix correlation between P and design matrices for limb elements, head shape, and lamellae, and the significance values for these correlations. Ecomorph category is indicated in parentheses (CG = crown-giant; GB = grass-bush; T = trunk; TC = trunk-crown; TG = trunk-ground; and TW = twig). Significant correlations by Mantel (1967) permutation tests are in bold. The three trunk-ground species are listed first.

	Head limbs lamellae		Head limbs		Head lamellae		Limbs lamellae		Head		Limbs		Lamellae	
Species	r_M	P	r_M	P	r_M	P	r_M	P	r_M	P	r_M	P	r_M	P
A. cybotes (TG)	**0.739**	**0.0002**	**0.737**	**0.0001**	0.198	0.1436	**0.668**	**0.0006**	0.209	0.1698	**0.668**	**0.0018**	0.030	0.7960
A. gundlachi (TG)	**0.701**	**0.0005**	**0.676**	**0.0004**	**0.261**	**0.0393**	**0.621**	**0.0003**	0.227	0.1051	**0.597**	**0.0041**	0.121	0.4264
A. sagrei (TG)	**0.739**	**0.0001**	**0.754**	**0.0002**	0.151	0.3184	**0.675**	**0.0005**	0.193	0.2281	**0.692**	**0.0012**	0.034	0.7938
A. baleatus (CG)	**0.643**	**0.0006**	**0.656**	**0.0003**	0.204	0.1391	**0.550**	**0.0043**	0.253	0.0687	**0.565**	**0.0050**	0.031	0.8170
A. chlorocyanus (TC)	**0.648**	**0.0002**	**0.661**	**0.0003**	0.212	0.1264	**0.552**	**0.0049**	**0.259**	**0.0406**	**0.566**	**0.0060**	0.029	0.8242
A. distichus (T)	**0.576**	**0.0002**	**0.558**	**0.0003**	**0.342**	**0.0164**	**0.443**	**0.0080**	**0.339**	**0.0277**	**0.425**	**0.0153**	0.090	0.4682
A. insolitus (TW)	**0.477**	**0.0004**	**0.466**	**0.0005**	**0.387**	**0.0058**	**0.310**	**0.0142**	**0.409**	**0.0099**	**0.298**	**0.0185**	0.059	0.6168
A. semilineatus (GB)	**0.657**	**0.0003**	**0.663**	**0.0002**	**0.461**	**0.0018**	**0.443**	**0.0073**	**0.528**	**0.0045**	**0.449**	**0.0083**	0.001	0.9737

Table 4. Principal component eignvectors from the 14-trait pooled phenotypic VCV matrix (pooled P) that was used for interspecies analyses. Eigenvalues, percentage of variation, and among-species variances (means and contrasts) for each eigenvector are at the bottom.

Trait	1	2	3	4	5	6	7	8	9	10	11	12	13	14
Head width	0.22	0.18	0.03	0.01	0.19	0.32	−0.01	−0.13	0.04	−0.48	−0.57	−0.08	0.19	−0.42
Head length	0.16	0.08	0.09	−0.01	0.15	0.21	0.01	−0.08	0.02	−0.26	−0.21	0.10	−0.40	0.78
Head height	0.27	0.22	0.12	−0.01	0.45	0.58	0.06	0.07	0.09	0.43	0.35	0.01	0.07	−0.06
Lamellae third foretoe	0.07	0.11	0.67	0.35	−0.32	0.01	−0.13	−0.52	−0.10	0.10	0.06	−0.01	0.04	−0.02
Lamellae fourth hindtoe	0.03	0.12	0.36	0.29	−0.27	0.04	0.08	0.76	0.32	−0.05	−0.10	−0.02	0.01	0.02
Pectoral width	0.27	0.38	−0.03	0.38	0.47	−0.63	0.02	0.03	−0.06	0.00	0.01	0.04	0.07	0.04
Humerus	0.29	−0.01	0.04	−0.19	−0.01	−0.12	−0.33	−0.02	0.29	−0.27	0.35	−0.62	−0.28	−0.10
Ulna	0.27	−0.10	0.26	−0.34	0.02	−0.05	−0.30	0.33	−0.69	0.03	−0.07	−0.07	0.20	0.09
Phalanx I third foretoe	0.44	−0.55	−0.31	0.58	−0.10	0.16	−0.07	0.03	−0.15	−0.05	0.08	0.03	0.00	−0.01
Pelvis width	0.36	0.58	−0.40	−0.07	−0.57	0.07	0.11	−0.03	−0.15	0.08	0.04	0.03	−0.03	0.02
Femur	0.25	−0.08	0.01	−0.22	−0.08	−0.09	−0.21	−0.09	0.41	−0.21	0.21	0.41	0.59	0.21
Tibia	0.25	−0.08	0.13	−0.20	0.00	−0.12	−0.12	0.04	0.06	0.02	0.00	0.61	−0.57	−0.38
Phalanx I fourth hindtoe	0.30	−0.20	−0.01	−0.16	−0.05	−0.17	−0.03	−0.10	0.32	0.60	−0.54	−0.20	0.02	0.08
Phalanx II fourth hindtoe	0.29	−0.21	0.23	−0.21	−0.02	−0.13	0.84	−0.06	−0.05	−0.15	0.13	−0.09	0.04	−0.02
Eigenvalues	0.0160	0.0060	0.0047	0.0046	0.0039	0.0034	0.0031	0.0022	0.0020	0.0015	0.0013	0.0009	0.0007	0.0006
Percentage of variation	31.45	11.71	9.31	8.96	7.60	6.70	6.14	4.34	3.95	2.91	2.55	1.80	1.43	1.15
Among-species variances (means)	0.1963	0.0294	0.0282	0.0326	0.0139	0.0111	0.0065	0.0040	0.0092	0.0047	0.0048	0.0068	0.0013	0.0049
Among-species variances (contrasts)	0.2311	0.0299	0.0433	0.0383	0.0176	0.0142	0.0103	0.0053	0.0108	0.0056	0.0064	0.0077	0.0019	0.0057

which supports the hypothesis of selection-driven convergence of **P**. The species for which we estimated **P** in this study are not particularly phylogenetically closely related (Fig. 1). In fact, several comparisons between species' **P** matrices span the deepest nodes in the *Anolis* phylogeny (Nicholson et al. 2005). Thus, the lack of a phylogenetic effect on **P** may be exacerbated by the deep divergences among species in this study in addition to convergence in **P** between the trunk-ground species. Questions concerning the temporal decay of the relationship between phylogeny and **P** could be addressed within clades of closely related species, such as the geographically widespread and genetically structured *Anolis cybotes* group (Glor et al. 2003).

Few comparable studies of **P** (or **G**) with a priori expectations for convergence exist, particularly ones conducted in a phylogenetic context. Similar to this study, Marroig and Cheverud (2001) found no correlation between divergence in **P** and phylogenetic distance at the generic level in New World monkeys, but found that differences in **P** were correlated with differences in feeding ecology. Along the same lines, phenotypic covariances for eye and antennal components differed in replicated pairs of spring versus cave-dwelling amphipod populations (Fong 1989; Roff 2002), suggesting that selective regimes associated with different environments can shape patterns of covariance during divergence in phenotypic mean trait values. Similarly, populations of calopterygid damselflies of distantly related species, but that were geographically close, converged in **P** (Eroukhmanoff et al. 2009), suggesting a response of wing morphology to common elements of an adaptive landscape. In contrast, the pattern of **G**-matrix variation was not related to phylogenetic relationships or morphological trait values among seven cricket species (Begin and Roff 2004), but in that case no a priori expectation for morphological convergence existed. Furthermore, Game and Caley (2006) found high **P** correlation and shared phenotypic covariance structure for comparisons between two populations within each of six distantly related fish species, but **P** was unrelated in comparisons between different species at the same geographic location. Thus, although results are somewhat mixed, it appears selective regimes associated with different environments can shape **P**. Two clear directions in which to extend this study are, first, obtaining estimates of **P** for multiple *Anolis* species from other ecomorph classes. This would strengthen the test for convergence of trait covariances and would increase the power to detect similarities within and differences among adaptive classes (ecomorphs). Second, the finding of **P** convergence increases our confidence in the utility of estimating **G**-matrices for these same species to test for concordant patterns.

Although trunk-ground species showed greater similarity in **P** than comparisons of species in different ecomorph classes, matrix correlations for all species were moderate to high and between six and 18 eigenvectors (i.e., the full CPC model, in this case)

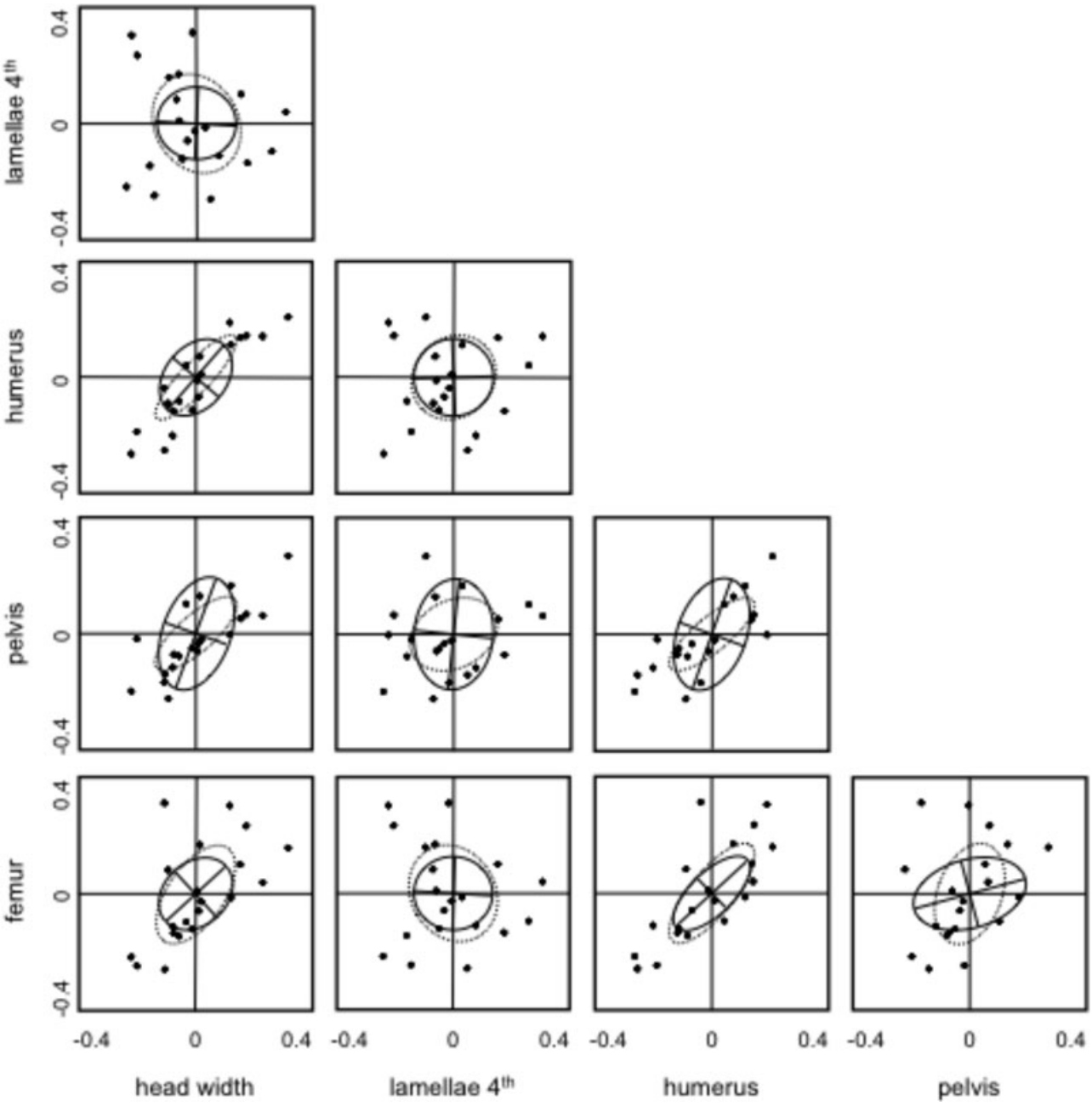

Figure 4. **The pattern of phenotypic variation and covariation within and among species for five traits: head width, lamella number, humerus length, pelvis width, and femur length, all after correcting for size. In each panel, the solid ellipse is a representation of the pooled within-species variation and covariation for the corresponding traits, whereas the broken ellipse is a representation of the pattern of among-species variation and covariation. As in Figure 3, the orientation of each ellipse is the primary eigenvector, whereas the length and width of each ellipse is proportional to two times the first and second eigenvalues, respectively. Among species variation and covariation was estimated from the phylogenetically independent contrasts, and the plotted points are all independent contrasts for the pair of traits. Within species ellipses (which were substantially smaller than among species ellipses in this study) were scaled by a factor of 6.05 to facilitate visual comparison of within and among species covariation. Note, however, that all analyses of these data were multivariate and these bivariate plots are only provided for convenience of visualization.**

were shared among these ecologically diverse and phylogenetically distant *Anolis* species. Furthermore, like the comparisons between trunk-ground species, all eight species shared full CPC with at least one other species in a different ecomorph class. In comparison, this same level of shared eigenstructure in **P** was found between two populations of Puerto Rican trunk-ground species *A. cristatellus* (Revell et al. 2007), whereas most other studies of **P** show that species share only the first two or three

Table 5. Results of the correlation tests for genetic drift using both species means and species independent contrasts. The number of species (*N*), Bartlett's test statistic and its associated degrees of freedom (df), and *P*-value (*P*) are shown. In addition, the highest individual correlation value (*r*) and its probability (*P*) along with the average value of all correlations (|*r*|) and PCs significantly correlated at $P = 0.05$. Asterisks indicate correlated PCs after Bonferroni correction of $P = 5.50 \times 10^{-4}$.

	N	Bartlett	df	*P*	*r*	*P*	Average |*r*|	Correlated PCs
Species (Means)	21	229.92	91	<0.0001	0.886	<0.0001	0.322	1−(2, 4, 6, 11, 14*) 2−(4*, 5, 6, 7, 8, 12, 14) 3−(5, 11) 4−(5, 10, 12*, 14) 6−(11, 12, 14) 7−(13) 9−(10*, 12) 10−(12)
Species (Contrasts)	21	227.60	91	<0.0001	0.861	<0.0001	0.325	1−(2, 4, 6, 8, 11, 14*) 2−(4*, 5, 6, 7, 8, 12, 14) 3−(5, 11) 4−(5, 9, 10, 12*) 6−(8, 11, 14) 7−(13) 8−(14) 9−(10*, 12*) 10−(12)

eignvectors (Steppan et al. 2002). In particular, Steppan (1997) never found common structure among species of *Phyllotis*, only among subspecies for some species. In our study, the first six eigenvectors of pooled **P** explained approximately 75% of morphological variation (Table 4). Thus, the orientations of eigenvectors explaining the majority of morphological variation were retained among many quite distantly related species. Equality and proportionality were rejected in all cases, but overall a high degree of shared phenotypic covariance structure exists for all eight species, which is consistent with the moderate-to-high matrix correlation values (Ackermann and Cheverud 2000).

Simulation studies have shown that numerous factors contribute to stability in the orientation of **G** including large population size, strong correlational selection, correlated pleiotropic mutation, the alignment of correlational selection and mutation, and their alignment with the direction of peak movement (Jones et al. 2003, 2004). Data for effective population sizes are not available for the species sampled here or any other *Anolis* species, but densities and census sizes are often quite high (reviewed in Losos 2009). It is plausible that some mutations have correlated effects on traits, such as the humerus and femur, but we have no data on mutational effects. On the other hand, we detected comparative evidence of correlational selection among PC axes in this study (Table 5), and field studies have found correlational selection on limb elements in male *A. sagrei* (Calsbeek and Smith 2007). The positive covariation among limb elements is a particularly stable component of **P** (Tables 3 and 4; Figs. 3 and 4), and the hypothesis follows that strong correlational selection on limb elements could contribute to this pattern.

PATTERN OF AMONG-TRAIT PHENOTYPIC INTEGRATION

Patterns of **P** in each species showed that some functionally based character sets are more integrated than others (Table 3). For example, some trait-pairs have highly conserved eigenstructure among species (e.g., humerus-femur), whereas covariances of traits from different character sets differed considerably among the species (Fig. 3). The integration of limb elements is not surprising given their shared function during locomotion; however, the pattern among ecomorphs suggests that differences in ecology may influence the degree of integration. The three trunk-ground species (*A. cybotes*, *A. gundlachi*, and *A. sagrei*) had the strongest correlations for limbs (Table 3). Trunk-ground ecomorph species have the longest relative limb length, fastest sprint speed, and run and jump more often than members of other ecomorph classes (reviewed in Losos 2009). Morphological integration of head shape is strongest in *A. insolitus* (twig) and *A. semilineatus* (grass-bush). Three-dimensional head shape analysis shows overlap for these ecomorphs, which have longer, narrower, and flatter heads compared to other ecomorphs (Harmon et al. 2005). These more streamlined heads may allow these species to more easily move through cluttered vegetation (Mattingly and Jayne 2004), and grass-bush and some twig anoles live in more cluttered habitats than other ecomorphs (Johnson 2007). Numerous developmental, genetic, and

functional factors could contribute to these patterns of integration, but one hypothesis for integration derived from the adaptive landscape that is amenable to testing in *Anolis* is correlational selection, which empirical and theoretical evidence suggests can lead to the evolution of genetic correlations between traits (Lande 1980b, 1984; Cheverud 1984; Brodie 1992; Calsbeek and Smith 2007).

Several recent studies have measured selection in *Anolis* lizard populations (Losos et al. 2004, 2006; Thorpe et al. 2005; Calsbeek and Irschick 2007; Calsbeek and Smith 2007, 2008; Revell et al. 2010), demonstrating its feasibility and suggesting measures of the multivariate adaptive landscape could be incorporated explicitly into analyses of phenotypic evolution in this system. Most studies have focused on the relationship between variation in morphological traits (e.g., body size, limb length) and survival using the truck-ground species *A. sagrei*. For limbs in particular, clearly some level of integration is needed to maintain locomotor abilities because mismatched limbs can negatively affect locomotion and potentially fitness (e.g., Martín and López 2001). The well-studied relationship between limb length and perch diameter—lizards with longer limbs run faster on broad surfaces, whereas those with shorter limbs are more adept on narrower surfaces (Losos and Sinervo 1989; Irschick and Losos 1999; Spezzano and Jayne 2004)—provides a strong functional link for selection studies. Calsbeek and Smith (2007) found correlational selection on limb elements in male *A. sagrei*. The form of selection was disruptive, favoring male lizards possessing long fore and hindlimbs as well as those with short fore and hindlimbs. These trait combinations corresponded to alternative broad and narrow perch diameters, respectively, and are consistent with the well-studied limb length-perch diameter relationship in *A. sagrei*. Additionally, Revell et al. (2010) found some support for the congruence of nonlinear selection and **P** in the trunk-ground anole, *A. cristatellus*, suggesting natural selection may have influenced the evolution of genetic architecture in this species. Unfortunately, most individual selection coefficients obtained by Revell et al. were not significantly different from zero, precluding an explicit analysis of "selective lines of least resistance" with a well-estimated adaptive landscape for divergence patterns in this study (Arnold et al. 2008; Hohenlohe and Arnold 2008). Estimates of multivariate selection surfaces are, however, a feasible goal in the *Anolis* system. Correlational selection on limb elements exists for one species of the long-limbed, fast moving, and frequently running and jumping trunk-ground ecomorph (Losos 1990; Calsbeek and Smith 2007), which could affect the genetic architecture of these traits. Determining if different ecomorph species experience differences in correlational selection that could lead to the observed patterns of integration among ecomorphs is key to testing functional hypotheses for integration.

INTEGRATION AND SPECIES DIVERGENCE

We found a strong correlation between pooled **P** and **D** (and $\mathbf{D_{IC}}$), showing alignment of patterns of covariances and divergence of phenotypic means for the 21 *Anolis* species in this study. One interpretation is that adaptive divergence among species is constrained by the pattern of genetic covariances, **G**, given the assumption that **P** and **G** are correlated. However, if the adaptive landscape has been stable over long time scales, this stability could produce alignment of mutation (**M**-matrix) and inheritance (**G**) patterns with selection surfaces, causing alignment of **G** with the adaptive landscape (Jones et al. 2007; Arnold et al. 2008). We rejected genetic drift when restricting the regression analyses to the first six eigenvalues, suggesting a role for diversifying and/or stabilizing selection on some PC axes, and we found evidence of correlational selection on some eigenvectors. This pattern as a whole is inconsistent with divergence by genetic drift alone (Marroig and Cheverud 2004; Table 5). To untangle the causal factors underlying the alignment of **P** and **D**, we would also need estimates of **G** to verify whether our substitution of **P** is appropriate for the species in our analyses and obtain estimates of multivariate selection surfaces. Hohenlohe and Arnold (2008) proposed a hypothesis-testing framework for microevolutionary inference from patterns of divergence based on maximum likelihood to address such questions. Unfortunately, their program, MIPoD, cannot be used to evaluate more than a few traits at this time, but their approach holds much promise for future investigations. In particular, when appropriate estimates of selection are available, direct evaluation of the correspondence between nonlinear selection surfaces and phenotypic divergence (**D**) will undoubtedly help to clarify this issue (Hohenlohe and Arnold 2008).

Trait combinations differ in how closely their divergence corresponds to dimensions of **P** (Fig. 4). Some trait combinations, such as humerus and femur, show strong positive covariation that matches closely the pattern of among-species divergence. In other instances, the within- and among-species patterns show less alignment, such as for humerus and pelvis or femur and pelvis (Fig. 4). Jones et al. (2003) found that strong correlational selection promotes stability, which is certainly plausible for limb elements in *Anolis* (Calsbeek and Smith 2007). What is unclear is how selection acts on other combinations of traits, and how this might vary among species, but we predict that limbs will show the strongest correlational selection, especially in trunk-ground species, and head shape characters will show stronger correlational selection in some species, particularly *A. insolitus* and *A. semilineatus*.

Conclusions

The species-rich and ecologically diverse genus *Anolis* provides an excellent opportunity to explore the role of genetic constraint

and the adaptive landscape in morphological diversification, and the repeated evolution of the ecomorphs presents a unique opportunity to test if convergence in the underlying pattern of phenotypic (and genetic) covariances accompanies multivariate phenotypic convergence. Our findings that trunk-ground ecomorphs have significantly higher pairwise correlations and more shared eigenvectors (Tables 1 and 2) and the highest levels of morphological integration for limbs (Table 3) suggest natural selection shapes patterns of covariance among traits in *Anolis* ecomorphs, revealing a previously undocumented dimension of convergence in this group. This evidence for convergence of **P** would be bolstered by future studies that include multispecies samples from other ecomorph classes. Less clear is whether the correspondence of pooled **P** with the divergence of phenotypic means for 21 *Anolis* species better reflects genetic constraint or evolution of **G** on a stable adaptive landscape.

ACKNOWLEDGMENTS

We thank the following individuals and institutions for help obtaining museum specimens: J. Simmons and L. Trueb, University of Kansas Natural History Museum; J. Rosado and J. Hanken, Harvard University Museum of Comparative Zoology; R. Powell, Avila University; and R. Glor, University of Rochester. We thank M. Alfaro, S. Arnold, J. McGlothlin, and an anonymous reviewer for comments. LJR was supported by the National Evolutionary Synthesis Center (NSF #EF-0423641) during the preparation of this manuscript. This work is supported by the National Science Foundation (DEB-0519777 & DEB-0519658).

LITERATURE CITED

Ackermann, R. R., and J. M. Cheverud. 2000. Phenotypic covariance structure in Tamarins (Genus *Saguinus*): a comparison of variation patterns using matrix correlation and common principal component analysis. Am. J. Phys. Anthropol. 111:489–501.

Agrawal, A. F., E. D. Brodie, III, and L. H. Rieseberg. 2001. Possible consequences of genes of major effect: transient changes in the G-matrix. Genetica 112:33–43.

Akaike, H. 1973. Information theory and an extension of the maximum-likelihoodprinciple. Pp. 267–281 *in* B.N. Petrov, and F. Csaki, eds. Second international symposium of information theory. Akademiai Kiado, Budapest, Hungary.

Arnold, S. J. 1992. Constraints of phenotypic evolution. Am. Nat. 140:S85–S107.

Arnold, S. J., M. E. Pfrender, and A. G. Jones. 2001. The adaptive landscape as a conceptual bridge between micro- and macroevolution. Genetica 112–113:9–32.

Arnold, S. J., R. Burger, P. A. Hohenlohe, B. C. Ajie, and A. G. Jones. 2008. Understanding the evolution and stability of the G-matrix. Evolution 62:2451–2461.

Baker, R. H., and G. S. Wilkinson. 2003. Phylogenetic analysis of correlation structure in stalk-eyed flies (*Diasemopsis diopsidae*). Evolution 57:87–103.

Bégin, M., and D. A. Roff. 2003. The constancy of the G matrix through divergence and the effects of quantitative genetic constraints on phenotypic evolution: a case study in crickets. Evolution 57:1107–1120.

———. 2004. From micro- to macroevolution through quantitative genetic variation: positive evidence from field crickets. Evolution 58:2287–2304.

Björklund, M. 1996. The importance of evolutionary constraints in ecological time scales. Evol. Ecol. 10:423–431.

———. 2004. Constancy of the G matrix in ecological time. Evolution 58:1157–1164.

Blows, M. W., and M. Higgie. 2003. Genetic constraints on the evolution of mate recognition under natural selection. Am. Nat. 161:240–253.

Blows, M. W., S. F. Chenoweth, and E. Hine. 2004. Orientation of the genetic variance-covariance matrix and the fitness surface for multiple male sexually selected traits. Am. Nat. 163:329–340.

Brodie, E. D., III. 1992. Correlational selection for color pattern and antipredator behavior in the garter snake *Thamnophis ordinoides*. Evolution 46:1284–1298.

Burnham, K. P., and D. R. Anderson. 2002. Model selection and multimodel inference: a practical information-theoretic approach. Springer, New York, NY.

Butler, M. A., and J. B. Losos. 2002. Multivariate sexual dimorphism, sexual selection, and adaptation in Greater Antillean Anolis lizards. Ecol. Monogr. 72:541–559.

Calsbeek, R., and D. J. Irschick. 2007. The quick and the dead: correlational selection on morphology, performance, and habitat use in island lizards. Evolution 61:2493–2503.

Calsbeek, R., and T. B. Smith. 2007. Probing the adaptive landscape using experimental islands: density-dependent natural selection on lizard body size. Evolution 61:1052–1061.

———. 2008. Experimentally replicated disruptive selection on performance traits in a Caribbean lizard. Evolution 62:478–484.

Chernoff, B., and P. Magwene. 1999. Morphological integration: forty years later. Pp. 319–353 *in* E. C. Olson and R. L. Miller, eds. Morphological integration. Univ. of Chicago Press, Chicago, IL.

Cheverud, J. M. 1984. Quantitative genetics and developmental constraints on evolution by selection. J. Theor. Biol. 110:155–171.

———. 1988. A comparison of genetic and phenotypic correlations. Evolution 42:958–968.

———. 1995. Morphological integration in the saddle-back tamarin (*Saguinus fuscicollis*) cranium. Am. Nat. 145:63–89.

———. 1996. Quantitative genetic analysis of cranial morphology in the cotton-top (*Saguinus oedipus*) and saddle-back (*S. fuscicollis*) tamarins. J. Evol. Biol. 9:5–42.

Cheverud, J. M., and G. Marroig. 2007. Comparing covariance matrices: random skewers method compared to the common principal components model. Genet. Mol. Biol. 30:461–469.

Cheverud, J. M., J. J. Rutledge, and W. R. Atchley. 1983. Quantitative genetics of development: genetic correlations among age-specific trait values and the evolution of ontogeny. Evolution 37:895–905.

Dietz, E. J. 1983. Permutation tests for association between two distance matrices. Syst. Zool. 32:21–26.

Eroukhmanoff, F., D. Outomuro, F. J. Outomuro, F. J. Ocharan, and E. I. Svensson. 2009. Patterns of phenotypic divergence in wing covariance structure of caloterygid damselflies. Evol. Biol. 36:214–224.

Farris, J. S. 1967. The meaning of the relationship and taxonomic procedure. Syst. Zool. 16:44–51.

Felsenstein, J. 1985. Phylogenies and the comparative method. Am. Nat. 125:1–15.

Flury, B. K. 1987. A hierarchy of relationships between covariance matrices. Pp. 31–43 *in* A. K. Gupta, ed. Advances in multivariate models. Wiley, New York, NY.

Fong, D. W. 1989. Morphological evolution of the amphipod Gammarus minus in caves: quantitative genetic analysis. Am. Mid. Nat. 121:361–378.

Game, E. T., and M. J. Caley. 2006. The stability of **P** in coral reef fishes. Evolution 60:814–823.

Glor, R. E., J. J. Kolbe, R. Powell, A. Larson, and J. B. Losos. 2003. Phylogenetic analysis of ecological and morphological diversification in Hispaniolan trunk-ground anoles (*Anolis cybotes* group). Evolution 57:2383–2397.

Hadfield, J. D., A. Nutall, D. Osorio, and I. P. F. Owens. 2007. Testing the phenotypic gambit: phenotypic, genetic and environmental correlations of colour. J. Evol. Biol. 20:549–557.

Harmon, L. J., J. J. Kolbe, J. M. Cheverud, and J. B. Losos. 2005. Convergence and the multidimensional niche. Evolution 59:409–421.

Hohenlohe, P. A., and S. J. Arnold. 2008. MIPoD: a hypothesis-testing framework for microevolutionary inference from patterns of divergence. Am. Nat. 171:366–385.

Irschick, D. J., and J. B. Losos. 1999. Do lizards avoid habitats in which performance is submaximal? The relationship between sprinting capabilities and structural habitat use in Caribbean anoles. Am. Nat. 154:293–205.

JMP, Version 8.0.2. 2009. SAS Institute Inc., Cary, NC.

Johnson, M. A. 2007. Behavioral ecology of Caribbean *Anolis* lizards: a comparative approach., Ph.D. Dissertation, Washington University in St. Louis.

Jones, A. G., S. J. Arnold, and R. Bürger. 2003. Stability of the G-matrix in a population experiencing pleiotropic mutation, stabilizing selection, and genetic drift. Evolution 57:1747–1760.

———. 2004. Evolution and stability of the G-matrix on a landscape with a moving optimum. Evolution 58:1639–1654.

———. 2007. The mutation matrix and the evolution of evolvability. Evolution 61:727–745.

Johnson, M. A., L. J. Revell, and J. B. Losos. 2010. Behavioral convergence and adaptive radiation: effects of habitat use on territorial behavior in Anolis lizards. Evolution 64:1151–1159.

Kolbe, J. J., R. E. Glor, L. Rodríguez Schettino, A. R. Chamizo Lara, A. Larson, and J. B. Losos. 2004. Genetic variation increases during biological invasion by a Cuban lizard. Nature 431:177–181.

Kolbe, J. J., A. Larson, and J. B. Losos. 2007. Differential admixture shapes morphological variation among invasive populations of the lizard *Anolis sagrei*. Mol. Ecol. 16:1579–1591.

Lande, R. 1979. Quantitative genetic analysis of multivariate evolution, applied to brain: body size allometry. Evolution 33:402–416.

———. 1980a. Sexual dimorphism, sexual selection, and adaptation in polygenic characters. Evolution 34:292–305.

———. 1980b. The genetic covariance between characters maintained by pleiotropic mutations. Genetics 94:203–215.

———. 1984. The genetic correlation between characters maintained by selection, linkage, and inbreeding. Genet. Res. 44:309–320.

Lande, R., and S. J. Arnold. 1983. The measurement of selection on correlated characters. Evolution 37:1210–1226.

Langerhans, R. B., J. H. Knouft, and J. B. Losos. 2006. Shared and unique features of diversification in Greater Antillean *Anolis* ecomorphs. Evolution 60:362–369.

Losos, J. B. 1990. Ecomorphology, performance capability, and scaling of West Indian *Anolis* lizards: an evolutionary analysis. Ecol. Monogr. 60:369–388.

———. 2009. Lizards in an evolutionary tree: ecology and adaptive radiation of anoles. Univ. of California Press, Berkeley, CA.

Losos, J. B., and B. Sinervo. 1989. The effects of morphology and perch diameter on sprint performance of *Anolis* lizards. J. Exp. Biol. 145:23–30.

Losos, J. B., T. W. Schoener, and D. A. Spiller. 2004. Predator-induced behaviour shifts and natural selection in field-experimental lizard populations. Nature 432:505–508.

Losos, J. B., T. W. Schoener, R. B. Langerhans, and D. A. Spiller. 2006. Rapid temporal reversal in predator-driven natural selection. Science 314:111.

Lynch, M., and B. Walsh. 1998. Genetics and analysis of quantitative traits. Sinauer, Sunderland, MA.

Mahler, D. L., L. J. Revell, R. E. Glor, and J. B. Losos. 2010. Ecological opportunity and the rate of morphological evolution in the diversification of Greater Antillean anoles. Evolution 64:2731–2745.

Manly, B. F. J. 2005. Multivariate statistical methods: a primer. Chapman & Hall, New York, NY.

Mantel, N. 1967. The detection of disease clustering and a generalized regression approach. Cancer Res. 27:209–220.

Marroig G., and J. M. Cheverud. 2001. A comparison of phenotypic variation and covariation patterns and the role of phylogeny, ecology, and ontogeny during cranial evolution of New World monkeys. Evolution 55:2576–2600.

———. 2004. Did natural selection or genetic drift produce the cranial diversification of neotropical monkeys? Am. Nat. 163:417–428.

Marroig, G., M. de Vivo, and J. M. Cheverud. 2004. Cranial evolution in sakis (*Pithecia*, Platyrrhini) II: evolutionary processes and morphological integration. J. Evol. Biol. 17:144–155.

Martín, J., and P. López. 2001. Hindlimb asymmetry reduces escape performance in the lizard *Psammodromus algirus*. Physiol. Biochem. Zool. 74:619–624.

Mattingly, W. B., and B. C. Jayne. 2004. Resource use in arboreal habitats: structure affects locomotion of four ecomorphs of *Anolis* lizards. Ecology 85:1111–1124.

McGlothlin, J. W., P. G. Parker, V. Nolan Jr., and E. D. Ketterson. 2005. Correlational selection leads to genetic integration of body size and an attractive plumage trait in dark-eyed juncos. Evolution 59:658–671.

McGuigan, K. 2006. Studying phenotypic evolution using multivariate quantitative genetics. Mol. Ecol. 15:883–896.

Meacham, C. A. 1993. MorphoSys: an interactive machine vision program for the acquisition of morphometric data. Pp. 393–402 *in* R. Fortuner, ed. Advances in computer methods for systematic biology: artificial intelligence, databases, computer vision. Johns Hopkins Univ. Press, Baltimore, MD.

Merilä, J., and M. Björklund. 1999. Population divergence and morphometric integration in the green-finch (*Carduelis chloris*) – evolution against the trajectory of least resistance. J. Evol. Biol. 12:103–112.

———-. 2004. Phenotypic integration as a constraint and adaptation, Pp. 107–129 *in* M. Pigliucci and K. Preston, eds. Phenotypic integration: studying the ecology and evolution of complex phenotypes. Oxford Univ. Press, Oxford, UK.

Nicholson, K. E., R. E. Glor, J. J. Kolbe, A. Larson, S. B. Hedges, and J. B. Losos. 2005. Mainland colonization by island lizards. J. Biogeogr. 32:929–938.

Olson, E. C., and R. L. Miller. 1958. Morphological integration. Univ. of Chicago Press, Chicago, IL.

Phillips, P. C. and S. J. Arnold. 1999. Hierarchical comparison of genetic variance-covariance matrices. I. Using the Flury hierarchy. Evolution 53:1506–1515.

Phillips, P. C., M. C. Whitlock, and K. Fowler. 2001. Inbreeding changes the shape of the genetic covariance matrix in *Drosophila melanogaster*. *Genetics* 158:1137–1145.

Revell, L. J. 2007a. The G matrix under fluctuating correlational mutation and selection. Evolution 61:1857–1872.

———. 2007b. Testing the genetic constraint hypothesis in a phylogenetic context: a simulation study. Evolution 61:2720–2727.

Revell, L. J., and L. J. Harmon. 2008. Testing quantitative genetic hypotheses about the evolutionary rate matrix for continuous characters. Evol. Ecol. Res. 10:311–321.

Revell, L. J., L. J. Harmon, R. B. Langerhans, and J. J. Kolbe. 2007. A phylogenetic approach to determining the importance of constraint on phenotypic evolution in the neotropical lizard *Anolis cristatellus*. Evol. Ecol. Res. 9:261–282.

Revell, L. J., D. L. Mahler, J. R. Sweeney, M. Sobotka, V. E. Fancher, and J. B. Losos. 2010. Nonlinear selection and the evolution of variances and covariances for continuous characters in an anole. J. Evol. Biol. 23:407–421.

Rice, W. R. 1989. Analyzing tables of statistical tests. Evolution 43:223–225.

Roff, D. A. 1995. The estimation of genetic correlations from phenotypic correlations: a test of Cheverud's conjecture. Heredity 74:481–490.

———. 1997. Evolutionary quantitative genetics. Chapman and Hall, New York, NY.

———. 2002. Comparing G matrices: a MANOVA approach. Evolution 56:1286–1291.

Schluter, D. 1996. Adaptive radiation along genetic lines of least resistance. Evolution 50:1766–1774.

———. 2000. The ecology of adaptive radiation. Oxford Univ. Press, Oxford, UK.

Spezzano, L. C., Jr., and B. C. Jayne. 2004. The effects of surface diameter and incline on the hindlimb kinematics of an arboreal lizard (*Anolis sagrei*). J. Exp. Biol. 207:2115–2131.

Steppan, S. J. 1997. Phylogenetic analysis of phenotypic covariance structure I. Contrasting results from matrix correlation and common principal component analysis. Evolution 51:571–586.

Steppan, S. J., P. C. Phillips, and D. Houle. 2002. Comparative quantitative genetics: evolution of the G matrix. Trends Ecol. Evol. 17:320–327.

Tallis, G. M., and P. Leppard. 1988. The joint effects of selection and assortative mating on multiple polygenic characters. Theor. Appl. Genet. 75: 278–281.

Thorpe, R. S., J. T. Reardon, and A. Malhotra. 2005. Common garden and natural selection experiments support ecotypic differentiation in the Dominican anole (*Anolis oculatus*). Am. Nat. 165:495–504.

Turelli, M. 1988. Phenotypic evolution, constant covariances, and the maintenance of additive variance. Evolution 42:1342–1347.

Williams, E. E. 1972. The origin of faunas. Evolution of lizard congeners in a complex island fauna: a trial analysis. Evol. Biol. 6:47–89.

———. 1983. Ecomorphs, faunas, island size, and diverse end points in island radiations of *Anolis*. Pp. 326–370 *in* R. B. Huey, E. R. Pianka, and T. W. Schoener, eds. Lizard ecology: studies of a model organism. Harvard Univ. Press, Cambridge, MA.

Willis, J. H., J. A. Coyne, and M. Kirkpatrick. 1991. Can one predict the evolution of quantitative characters without genetics? Evolution 45:441–444.

Associate Edior: M. Alfaro

Appendix1: Museum Specimens

Abbreviations for collections: BWMC, Bobby Witcher Memorial Collection, Avila University; KU, Museum of Natural History, University of Kansas; Losos Lab, Jonathan B. Losos Lab field series; MCZ, Museum of Comparative Zoology, Harvard University; REG, Richard E. Glor field series.

A. baleatus-KU 250754–250755, 250758, 250763–250765, 250767–250768, 250775–250776, 250778–250779, 250788–250802, 250807–250814, 250816–250817, 250819–250820, 250834–250840, 250846–250865, 250870, 250873–250874, 250878, 250883–250895; *A. chlorocyanus*-KU 250892–250895, 252158, 252163–252164, 252166, 252173, 252175, 252181, 252183–252184, 252187, 252189–252191, 252196–252198, 252202, 252207, 252210, 252217, 252220–252223, 252228–252229, 252232–252233, 252235–252240, 252242, 252253–252255, 252257, 252263–252267, 252269, 252273–252277, 252282, 252286–252289, 252293–252296, 252298–252302, 252305–252310, 252317–252321, 252328, 252330–252336, 252342, 252346–252347, 252349–252351, 252353, 252355, 252376–252377, 252380, 252383; *A. cybotes*-BWMC 2488, 3143–3144, 3148, 3151, 3534, 3536–3537, 3541, 3545–3549, 3562–3565, 3567, 3569, 3573, 3575–3577, 3579–3582, 4545–4546, 4548, 4550, 4552, 4556–4557, 4559, 5232–5234, 5254–5255, 5257–5258, 5261–5262, 5456, 5460, 5462–5463, 5483–5484, 6405, 6407–6408, 6581–6585, REG 402–403, 405, 408, 412–413, 417–418, 421–422, 425–426, 428, 446–447, 449–450, 452–455, 737–740, 755–763, 768–770, 773; *A. distichus*-KU 256277–256279, 256282–256286, 256288, 256292–256293, 256298, 256301, 256303, 256305–256306, 256308–256313, 256316–256318, 256320, 256324, 256326–256328, 256331–256333, 256336–256342, 256373, 256375, 256377–256379, 256381–256391, 256393–256394, 256396–256398, 256506, 256508–256509, 256513–256514, 256518, 256522–256523, 256527–256529, 256533, 256539, 256543, 256545–256546, 256824–256826, 256829, 256832, 256869, 256875, 256884–256885, 256889, REG 546–548, 550, 553–554, 566, 568, 570, 573–575, MCZ V20711, X8490, X9286; *A. gundlachi*-KU 257851–257855, 257857–257859, 257862, 257866–257879, 257881–257914, 257918–257925, 257927–257930, 257932–257935, 257938, 257943–257947; *A. insolitus*-KU 257764–257772, 257774–257784, 257787–257799, 257801, 257803–257807; *A. semilineatus*-KU 247350–247351, 247353, 247363–247368, 247374–247378, 247381, 247383, 247388–247391, 247400–247404, 247411–247414, 247419–247420, 247424–247428, 247430–247432, 247434, 247436, 247439, 247442, 247449–247456, 247458–247459, 247465–247467, 247469, 247472, 247479, 247482–247483, 247486, 247495, 247502–247503, 247524–247526, 247532, 247535, 247538–247547, 247550–247551, 247553, 247556–247561, 247563, 247572–247575, 247579–247582, 247585, 247588; *A. sagrei*-Losos Lab 15–16, 23–26, 33, 44–47, 49–56, 67–68, 71–81, 89–97, 115–230, 439, 441, 444, 446, 449, 452, 454, 457, 460–462, 464–465, 468, 472, 474, 476.